Measurement of the radiative lifetime of the $1s2s\ ^3S_1$ level in heliumlike magnesium

G. S. Stefanelli,[1] P. Beiersdorfer,[2] V. Decaux,[2] and K. Widmann[2]
[1]*Department of Physics, University of Nevada, Reno, Nevada 89557*
[2]*Lawrence Livermore National Laboratory, University of California, P.O. 808, Livermore, California 94550*
(Received 17 January 1995; revised manuscript received 16 June 1995)

We apply a recently developed electron-beam ion trap technique to measure the lifetime of the $1s2s\ ^3S_1$ level in heliumlike magnesium. The technique employs a fast-switching electron beam to produce and excite electrostatically trapped ions. The radiative lifetime is determined by observing the fluorescent decay of the $1s2s\ ^3S_1$ level after the beam energy is switched below the threshold for electron-impact excitation. A value of $13.61 \pm 0.49\ \mu$s has been measured for the $1s2s\ ^3S_1$ level in heliumlike magnesium, in good agreement with theoretical predictions.

PACS number(s): 32.70.Fw, 34.80.Kw, 95.30.Ky

Experimental measurements of the radiative lifetime of excited levels in heliumlike ions have provided important tests of theoretical atomic calculations. These tests include relativistic effects [1], two-photon decay [2], and the hyperfine interaction [3,4]. In addition, precise knowledge of the decay rate is important in the study of astrophysical and laboratory plasmas [5]. The $1s2s\ ^3S_1$ level was originally predicted to decay primarily through two-photon emission [6]. However, in spectral observations from the sun it was subsequently shown that a significant magnetic-dipole ($M1$) branch exists for the decay of the $1s2s\ ^3S_1$ level [7,8]. The lifetime of the $1s2s\ ^3S_1$ level in He-like ions has been under intense investigation ever since its identification in the solar spectrum. Accelerator beam-foil methods and photon-fluorescence techniques have been very successful in measuring radiative lifetimes in He-like ions for $Z \leq 3$ [9,10] (for which $\tau \geq 58.6$ sec) and $Z \geq 16$ [11–17] (for which $\tau \leq 706$ ns). However, the two methods have left a large gap for radiative lifetimes in multiply charged ions in an eight order-of-magnitude range which are too energetic for photoexcitation by flash tubes or lasers and are too slow to be measured with beam-foil techniques. This gap has been closed by the recent development of two experimental techniques. Storage rings have been used to measure the radiative lifetime of the $1s2s\ ^3S_1$ level in C^{4+} and N^{5+} for which $\tau = 20.60$ ms and $\tau = 3.905$ ms, respectively [18]. Moreover, an electron-beam ion trap (EBIT) has been used to measure the $1s2s\ ^3S_1$ lifetime in Ne^{8+} for which $\tau = 90.6\ \mu$s [19]. The latter technique can be used in principle to measure any $1s2s\ ^3S_1$ lifetime in the region $10^{-2}\ \text{s} \leq \tau \leq 10^{-7}$ s. In the following we used the EBIT technique to measure the 13.6-μs lifetime of the $1s2s\ ^3S_1$ level in Mg^{10+}.

In the recently developed EBIT technique the radiative lifetime for the $1s2s\ ^3S_1$ level in He-like Mg^{10+} is measured using high-resolution x-ray spectroscopy of stationary electrostatically trapped ions. Production and excitation of He-like Mg^{10+} occurs via impact with a monoenergetic electron beam. The electron-beam energy is fast switched between 1895 and 1200 eV, above and below the 1331-eV threshold for excitation of the $^3S_1$ level. The radiative lifetime is then determined by observing the temporal decay of the photon signal after the beam is switched below threshold.

The photon signal is analyzed using a vacuum flat-crystal spectrometer (FCS) in an arrangement shown in Fig. 1. The spectrometer employs a thallium-hydrogen-phthalate crystal ($2d = 25.9$Å) and a position-sensitive proportional counter. A description of the spectrometer is given in Ref. [20]. With the FCS we recorded the spectrum of the Mg^{10+} $n = 2$ to $n = 1$ transitions shown in Fig. 2. The electron-beam energy is at 1895 eV, i.e., above threshold for excitation of the $^3S_1$ level. This spectrum includes the resonance line w ($1s2p\ ^1P_1 \rightarrow 1s^2\ ^1S_0$), the intercombination blend of x and y ($1s2p\ ^3P_{2,1} \rightarrow 1s^2\ ^1S_0$), the forbidden line z ($1s2s\ ^3S_1 \rightarrow 1s^2\ ^1S_0$), and the lithiumlike resonance line q ($1s2s2p\ ^2P_{3/2} \rightarrow 1s^2 2s\ ^2S_{1/2}$). The $wxyz$ notation is that of Gabriel [21]. The xy blend is dominated by y since the $^3P_2$ level has only a 7% branching ratio for decay via x. The spectrum also shows a weak background line labeled B, which has not been identified. We believe that this line is due to ions indigenous to EBIT, such as barium, lanthanum, or

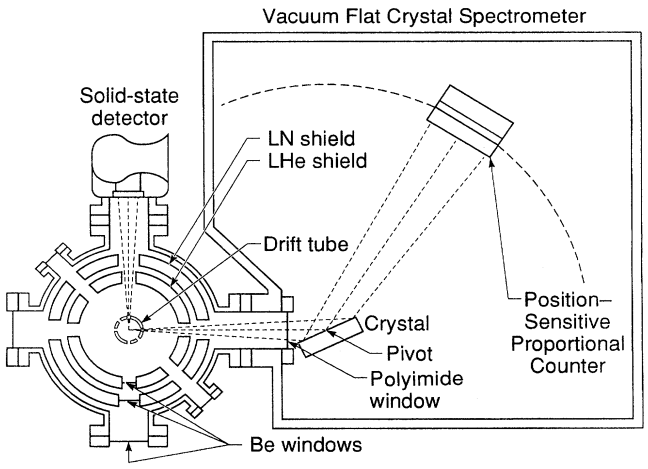

FIG. 1. Schematic layout of the vacuum flat-crystal spectrometer (FCS). The electron beam is directed out of the page. The crystal and position sensitive proportional counter rotate about a common pivot point. The spectrometer is attached to one of EBIT's six observation points, and uses a 1-μm-thick polyimide window to separate its vacuum from that of EBIT.

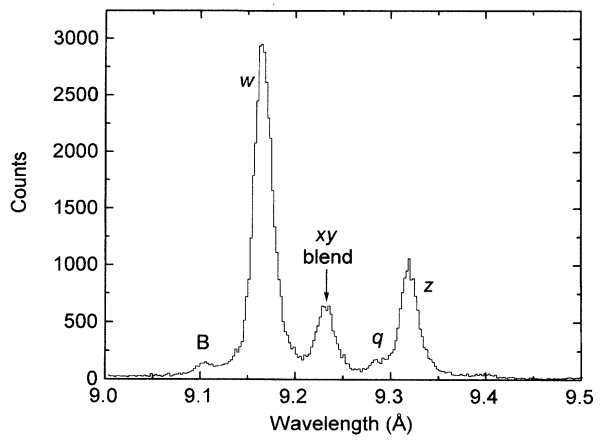

FIG. 2. K-shell spectrum of He-like Mg (FCS) includes the resonance line w, the blend of intercombination lines x and y, the forbidden line z, and the lithiumlike resonance line q. The line labeled B is produced by ions indigenous to EBIT.

tungsten. These elements are constantly introduced into EBIT from the filament of the electron gun. Line B was the only background line in the region of interest.

An event-mode data-acquisition system recorded the spectrum as a function of time with a resolution of 0.58 μs. A high-precision function generator provides timing for the fast-switching electron beam. The electron-beam energy as a function of time is shown in Fig. 3. Starting at 1895 eV we fast switch the electron-beam energy to 1200 eV. The shape of the beam-energy trace represents a compromise between the necessity for a fast pass through the electron-impact excitation threshold of z and the slew rate of the power supply. A slew rate of about 10 eV/μs at the point where the beam energy passes below the excitation threshold of z is achieved with the trace shown. Because of the 40–50-eV spread in energy of the beam electrons [22], it takes about 4–5 μs for the beam energy to sweep below a given threshold. An overshoot causes a brief dip of the energy into the range of the KLM resonances. The pattern repeats every 200 μs.

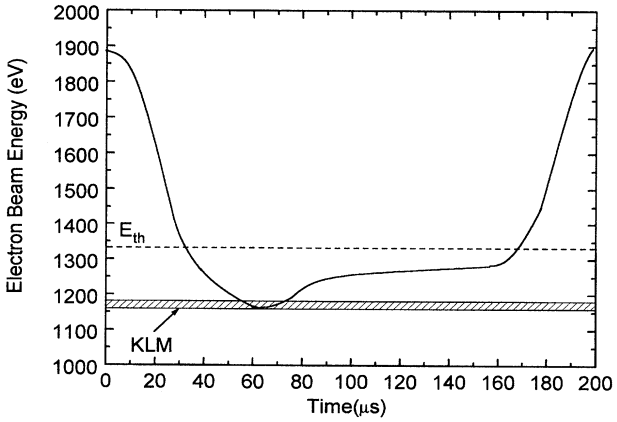

FIG. 3. Electron-beam energy as a function of time. Note the dip of electron beam energy into the KLM dielectronic recombination resonance.

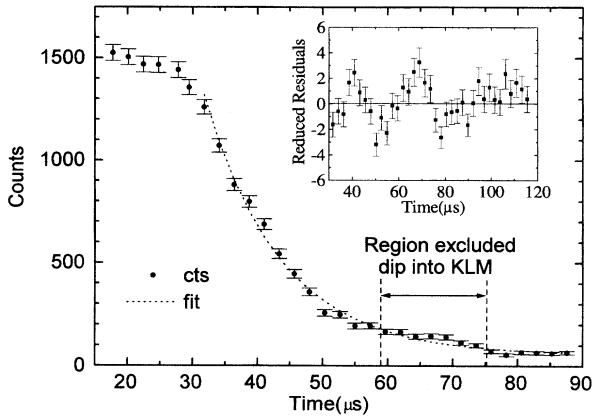

FIG. 4. Combined intensity as a function of time of xy and z recorded by the FCS. The electron beam energy falls below the threshold for electron-impact excitation of z near $t=33$ μs (cf. Fig. 2). The dotted line is a fit to an exponential term plus a constant background. In this fit the counts contributed by dielectronic recombination (DR) are excluded. Counts contributed by DR to the net photon signal are seen as a "bump" over the fit in region (58 μs $\leq t \leq$ 75 μs). A plot of the reduced residuals of the fit is shown as an inset.

As the beam energy sweeps below threshold for excitation, the emission from w and q cease essentially instantaneously. It is replaced by emission from satellite lines caused by dielectronic capture into the high-lying $1s2pnl$ or $1s2s2pnl$ with $n \geq 4$, whose energies are virtually the same as that of w or q [23,24]. By contrast, the emission from z and, as discussed below, from xy persists over an extended period of time and falls off exponentially. The exponential behavior of the temporal decay as the electron-beam energy falls below threshold for electron-impact excitation of z is evident. The temporal behavior of the combined intensity of xy and z measured with the FCS is shown in Fig. 4. Dielectronic recombination (DR) into $n=3$ (KLM) levels occurs when the electron-beam energy dips into the KLM resonance energy. During this time the observed emission of z is enhanced by photons produced by DR representing the $n=3$ satellites of q that blend with z and cannot be resolved by the FCS. A corresponding enhancement can be seen in the temporal decay curve (cf. Fig. 4). By contrast, the intensity of the background signal to either side of the region of interest did not show any temporal variation. The intensity of line B remained constant during this time.

Collisional transfer of an electron from the $1s2s\ ^3S_1$ level to the $1s2p\ ^3P_{2,1,0}$ levels occurs at the electron densities of the present measurement ($<10^{12}$ cm^{-3}) and must be considered. The $^3P_2$ and $^3P_0$ levels decay back to the $^3S_1$ level, but the $^3P_1$ level decays to ground via y photon emission. The collisional transfer is evident in Fig. 5 which shows a spectrum of the observed emission when the beam energy is lowered below the z excitation threshold. A small feature at the position of xy produced by collisional transfer from the $^3S_1$ level can be seen. The figure also shows satellites at the position of w and q produced by DR resonance's with $n \geq 4$.

Collisional transfer reduces the overall lifetime of the $^3S_1$ level. Following the procedure discussed in [19] effects

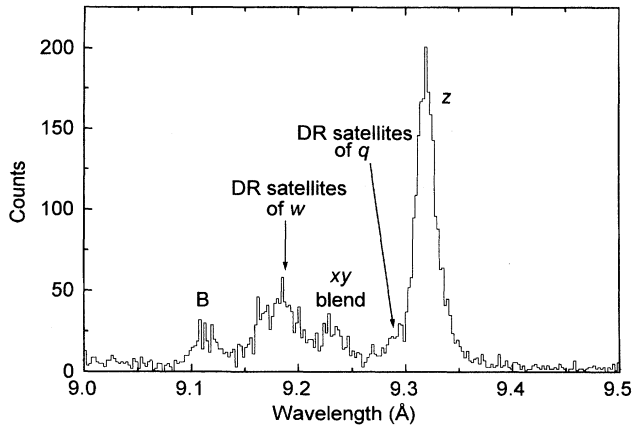

FIG. 5. Below threshold spectra of He-like Mg as seen by the FCS. Note how only xy and z remain when the beam energy is lowered below z's excitation threshold. In addition, satellite lines at the position of w and q are seen, which are produced by DR resonance's with $n \geq 4$. The line labeled B is produced by ions indigenous to EBIT (cf. Fig. 2).

of this collisional redistribution can be accounted for provided the relative intensity of y excited by the transfer is measured. Using the fact that the radiative lifetime of x (0.094 μs) and y (2.94×10^{-5} μs) [25] are short compared to that of z and that collisional redistribution from the $^3S_1$ level to any other levels that might decay to ground is insignificant we obtain

$$\tau_z = \tau_{\text{decay}}\left(1+\frac{I_{xy}}{I_z}\right), \tag{1}$$

where I_{xy} and I_z are line intensities during decay when the beam energy is lowered below threshold and τ_{decay} is the decay constant of the combined intensity curve which is a sum of the decay curves for xy and z. In other words, the radiative lifetime τ_z of z is equal to the decay constant of the combined intensity curve multiplied by a correction factor arising from the collisional redistribution of the $^3P_1$ level to $^3P_1$. The intensity ratio I_{xy}/I_z was obtained using the number of counts in the xy and z lines given by a least-squares line-fitting procedure when the electron-beam energy is lowered below the threshold for excitation of z (cf. Fig. 5). The ratio was determined in several spectra recorded at different times after the beam energy is lowered below threshold. This enabled us to assess possible contributions from satellites with $n \geq 4$. The average value found is $I_{xy}/I_z = 0.16 \pm 0.02$.

To determine τ_{decay} a nonlinear least-squares method is used to fit the decay curve shown in Fig. 4. For the fit we use a function of the form

$$I(t) = Ae^{-t/\tau_{\text{decay}}} + B, \tag{2}$$

i.e., an exponential term plus a constant background. The point at which the excitation of w ceases is taken as $t = t_0$. This point is determined by performing a linear fit to the "flat-top" of the decay curve. The flat top region is defined as counts(t) for $t_{\text{on}} < t < t_0$ with t_{on} being the point where at which the excitation of w begins. Since the energy distribution of the beam electrons is a Gaussian (40–50-eV energy spread), w can contribute a small number of counts to the decay curve for a short time (4–5 μs) after the beam is switched below threshold. We can eliminate any contribution from w by choosing t_0 to be the first point on the decay curve that differs from the linear fit by a 5% tolerance. The exponential term plus constant background is calculated two ways, including and excluding the times when the *KLM* dielectronic satellites of q contribute counts (cf. Fig. 4). The small error in the estimate of τ_{decay} due to satellite contributions is determined from the difference in the results obtained from the two fits. Reduced residuals for the fit are shown as an inset to Fig. 4. The reduced residual (R_{resid}) is defined as the actual number of counts at time t minus the value of the fit to decay curve at time t divided by the square root of the value of the fit (i.e., $R_{\text{resid}} = [N(t) - I(t)]/[I(t)]^{1/2}$). A value of 11.79 ± 0.31 μs is found for τ decay when including and 11.74 ± 0.31 μs is found when excluding the time of the satellite contributions. For the calculation of τ_z we use the latter value.

TABLE I. Experimental results for radiative lifetime measurement of the $1s2s\ ^3S_1$ level in heliumlike magnesium.

Quantity	Measurement
τ_{decay}	
Fit results	11.74 ± 0.31 (μs)
I_{xy}/I_z	
Fit results	0.16 ± 0.02
Resulting increase in τ_{decay}	1.87 ± 0.24 (μs)
Systematic errors (μs)	
Timing error	0.27
n_e profile	0.03
Line polarization	0.09
Ion loss	0.01
Blending of $n=3$ satellites of q	0.05
τ_z	
Final value	13.61 ± 0.49 (μs)

Several sources of systematic errors affecting our measurement exist. These include the effects of the variation of electron bean density with radius (n_e profile), the loss of $^3S_1$ states due to recombination or ion loss from the trap region, uncertainties in timing, and polarization effects. An overview of the estimated errors are given in Table I. Corrections for such effects have been calculated previously for He-like Ne^{8+} [19] and were found to be small. We make no such corrections for our data. For example, the error introduced by not accounting for polarization effects is estimated to be less than 0.09 μs and that due to variations in n_e profile is less than 0.03 μs.

Finally, the maximum electron energy in our measurements is sufficient to excite high-n Rydberg levels. Consequently, cascade contributions from these levels to the $^3S_1$ level are of concern. We calculated electron-impact excitation cross sections, radiative decay rates and channels of such levels and find that for $n > 4$ only levels of the type $1s\,np$ make significant contributions to the population of the $^3S_1$ level. Their decay rates are many orders of magnitude

larger than that of the $^3S_1$ level. For cascades from the $n=5$ shell, for example, the rates are 9.0×10^{10} s^{-1}, or six orders of magnitude faster than the radiative decay rates for the $^3S_1$ level. Corrections for slow radiative cascade contributions from high-n levels are thus not necessary.

The final value of τ_z is summarized in Table I. Its uncertainty is determined from quadrature addition of the statistical and systematic errors listed in Table I. The final result of 13.61 μs$\pm$0.49 μs is in good agreement with the 13.80-μs value calculated by Drake [26] and the 13.64-μs value calculated by Lin, Johnson, and Dalgarno [25].

We gratefully acknowledge contributions by A. Osterheld. Work performed at LLNL under the auspices of the U.S. Department of Energy under Contract No. W-7405-ENG-48. This research was supported in part by DOE-EPSCoR (Nevada), and the Office of Basic Energy Sciences–U.S. Department of Energy.

[1] R. Marrus *et al.*, Phys. Rev. A **39**, 3725 (1989).
[2] R. Marrus *et al.*, Phys. Rev. Lett. **56**, 1683 (1989); R. W. Dunford, *ibid.* **62**, 2809 (1989); Phys. Rev. A **38**, 5423 (1988).
[3] H. Gould, R. Marrus, and P. J. Mohr, Phys. Rev. Lett. **33**, 676 (1974).
[4] R. W. Dunford *et al.*, Phys. Rev. A **44**, 764 (1991).
[5] F. P. Keenan, in *UV and X-ray Spectroscopy of Laboratory and Astrophysical Plasmas*, edited by E. Silver and S. Kahn (Cambridge University Press, New York, 1993), p. 44.
[6] G. Breit and E. Teller, Astrophys. J. **91**, 215 (1940).
[7] A. H. Gabriel and C. Jordon, Nature (London) **221**, 947 (1969).
[8] H. K. Griem, Astrophys. J. **161**, L155 (1970).
[9] H. W. Moos and J. R. Woodworth, Phys. Rev. Lett. **30**, 775 (1973); J. R. Woodworth and H. W. Moos, Phys. Rev. A **12**, 2455 (1975).
[10] R. D. Knight and H. M. Prior, Phys. Rev. A **21**, 179 (1980).
[11] C. L. Cocke, B. Curnutte, and R. Randall, Phys. Rev. Lett. **31**, 507 (1973).
[12] J. R. Bednar *et al.*, Phys. Rev. A **11**, 460 (1975).
[13] H. Gould, R. Marrus, and R. W. Schmieder, Phys. Rev. Lett. **31**, 504 (1973).
[14] G. Hurbricht and E. Traebert, Z. Phys. D **7**, 243 (1987).
[15] R. W. Dunford *et al.*, Phys. Rev. A **41**, 4109 (1990).
[16] S. Cheng *et al.*, Phys. Rev. A **49**, 2347 (1994).
[17] A. Simionovici *et al.*, Phys. Rev. A **49** 3553 (1994).
[18] H. T. Schmidt *et al.*, Phys Rev. Lett. **72**, 1616 (1994).
[19] B. J. Wargelin, P. Beiersdorfer, and S. M. Kahn, Phys. Rev. Lett. **71**, 2196 (1993).
[20] P. Beiersdorfer and B. J. Wargelin, Rev. Sci. Instrum. **65**, 13 (1994).
[21] A. H. Gabriel, Mon. R. Astron. Soc. **160**, 99 (1972).
[22] M. A. Levine *et al.*, Nucl. Instrum. Methods Phys. Res. Sect. B **43**, 431 (1989).
[23] F. Bely-Dubau, A. H. Gabriel, and S. Volonte, Mon. R. Astron. Soc. **189**, 801 (1979).
[24] P. Beiersdorfer, *et al.*, Z. Phys. D **21**, 5209 (1991).
[25] C. D. Lin, W. R. Johnson, and A. Dalgarno, Phys. Rev. A **15**, 154 (1977).
[26] G. W. F. Drake, Phys. Rev. A **3**, 908 (1971).